Analysis of GPS Signal Acquisition Performance

* Xiaofan LI[1], Dinesh MANANDHAR[2], Ryosuke SHIBASAKI[3]

[1,3]Center for Spatial Information Science, The University of Tokyo
[2]GNSS Technologies Inc and Center for Spatial Information Science, The University of Tokyo
(E-mail: [1]xiaofan@iis.u-tokyo.ac.jp, [2]dinesh@gnss.co.jp, [3]shiba@csis.u-tokyo.ac.jp)

Abstract

Acquisition is to detect the presence of the GPS signal. Once the signal is detected, the estimated frequency and code phase are passed to a tracking loop to demodulate the navigation data. In order to detect the weak signal, multiple length of data integration is always needed. In this paper, we present five different acquisition approaches based on circular correlation and Fast Fourier Transform (FFT), using coherent as well as non-coherent integration techniques for the multiple length of collected GPS satellite signal. Moreover a general approach of determining the acquisition threshold is introduced based on noise distribution which has been proved effective, and independent of the hardware. In the end of this paper, the processing speed and acquisition gain of each method are illustrated, compared, and analyzed. The results show that coherent approach is much more time consuming compared to non-coherent approaches, and in the case of multiple length of data integration from 2ms to 8ms, the processing times consumed by the fastest non-coherent acquisition method are only 25.87% to 1.52% in a single search, and 34.76% to 1.06% in a global search of those in the coherent acquisition. However, coherent acquisition also demonstrates its better performance in the acquisition gain, and in the case of 8ms of data integration it is 4.23 to 4.41 dB higher than that in the non-coherent approaches. Finally, an applicable scheme of combining coherent and non-coherent acquisition approaches in the development of a real-time Software GPS receiver in the University of Tokyo is provided.

Keywords: GPS Signal, Acquisition, Software Receiver
.

1. Introduction

Acquisition is a main step in the design of GPS receiver, as to identify the visible satellites and find the beginning point of the C/A code as well as the Doppler frequency. In this paper, C programming codes are applied in Pentium IV 2.80GHz computer to evaluate the speed for a real time application. The GPS data in the experiment was collected by using the front-end, which has the sampling frequency of 16.3676MHz, and the Intermediate Frequency of which is at 4.1304MHz.

The purpose of this paper is to test and evaluate five common GPS C/A code acquisition algorithms. The speed and output signal-to-threshold ratio of each method are compared and evaluated. The signal detection threshold is also determined based on the noise probability density function.

2. Block Processing Approach

The GPS signal processing is treated as a block processing, that the signal is processed as a block of data rather than being processed sequentially. The block size is selected as the length of the C/A code period, says 1023 chips, at the chip rate of 1.023MHz for a time length of 1ms. The specification of the block processing in this paper is listed below:

•Standard Time Length	1ms
•Sampling Frequency	16.3676 MHz
•Block Size	1023chips/16368bits
•Time Resolution	61.1ns
•Doppler Range	[-6000,6000]Hz

3. Signal Model

The received signal logged by the front-end device can be expressed as:

$$S(t)=AC(t)D(t)\sin(2\pi(f_{IF} + f_{doppler})+q_0)+N(t) \qquad (1)$$

Where A is the GPS signal amplitude; C(t) is the PRN Code; D(t) is the navigation data, f_{IF} is the intermediate carrier frequency, 4.1304MHz; $f_{doppler}$ is the doppler frequency shift that is between -6000Hz to 6000Hz for a static receiver; q_0 is the phase offset and N(t) is the term of background noise. The input signal power can be calculated as $P_S = A^2 / 2$ and the noise power is denoted as $P_N = s_N^2$ where s_N^2 is the baseband average noise power, thus the signal-to-noise ratio (S/N) is expressed as $S/N = 10\log_{10}(A^2/2s_N^2)$ dB. By applying this function, it is fairly convenient to create simulated GPS data at various S/N ratios by specifying those two parameters. However as for the collected data, it is difficult to measure the input S/N ratio since A and s_N^2 are unknown. But, the intensity of different satellite signals can be differentiated later by computing the carrier-to-noise ratio (C/N_o), if the code phase, carrier frequency and phase are obtained from the acquisition [1].

4. Signal Processing Methods

In this section, five different acquisition approaches will be presented, all of which are designed for C/A code and able to process 1ms or a multiple length of data. The maximum data length for the acquisition is considered as 10ms in order to avoid navigation data transition.

In GPS signal acquisition, the Fast Fourier Transform is extremely essential, since it tremendously accelerates the speed of processing when compared with the conventional serial search method. If the length of FFT data is N, the power of 2, the complexity of the FFT calculation is $(N/2)\log_2(N)$ complex multiplication and N $\log_2(N)$ complex addition. However, since the length of sample data is 16368 which is not a 2^n number, then FFT routine with an arbitrary length is chosen in the experiment [2], which causes the calculation complexity to be larger.

The symbols used in the algorithm description are listed and explained below:

$g(t)$: GPS raw signal collected from the front end, which contains 16368 bits for 1ms of time length.

$ca(t)$: Local C/A (PRN) code of a certain satellite, totally 32 types and each contains 16368 bits for 1ms of time length.

$R_{IF}(t)$: Locally generated complex carrier wave at the intermediate frequency of 4.1304MHz. It contains 16368 bits for 1ms of time length, and is generated by $\exp(j*2pf_{IF}t)$.

$R_{Fdoppler}(t)$: Locally generated complex carrier wave at the frequency of specific satellites, considering the Doppler frequency. It contains 16368 bits for 1ms of time length, and is generated by $\exp(j*2p(f_{IF}+f_{doppler})t)$.

A. Standard Non-Coherent Circular Correlation[3]

Non-coherent integration is to acquire successive time slices of data but process them separately and sum their results together. The procedure of a standard non-coherent integration method is presented as follows:

1. Generate 13 different $R_{Fdoppler}(t)$ with the dopper frequencies from -6000Hz to 6000Hz at an interval of 1kHz.
2. Multiply $R_{Fdoppler}(t)$ with $ca(t)$ to generate the local signal $l(t)$.
3. Perform FFT on $l(t)$ and $g(t)$ to generate L(K) and G(K)
4. Take conjugate of G(K) and get CG(K)
5. Multiply L(K) and CG(K) and take IFFT to obtain 16368 complex outputs. This covers one Doppler frequency component.
6. Circular processing of 13 Doppler frequency components will be done, and the peak absolute value of totally 13×16368=212784 complex outputs will be compared to the predetermined threshold. The satellite is evaluated as visible if the former surpasses the latter.

This process will be repeated 32 times to implement a global search for all 32 satellites. For the case of integrating n ms of data, the length of $g(t)$ will become n×16368 bits, however the length of $l(t)$ and $ca(t)$ is still 16368 since this integration is non-coherent. Hence in the step 3, $g(t)$ will be calculated n times to obtain n ms of G(K), the outputs in step 5 will are summed for n ms to generate the final result, which is still 16368 bits. The FFT calculation complexity, frequency and time resolution of method A are listed in the table 1 of the next page.

B. Improved Non-Coherent Circular Correlation

This method is quite similar to method A, the only difference is to multiply $R_{Fdoppler}(t)$ with $g(t)$ instead of $ca(t)$ to generate one group $l(t)$, the other group is $ca(t)$, then perform FFT of each group to obtain L(K) and G(K). The rest of operation remains the same. The advantage of applying this method is that it dramatically decreases the FFT complexity in a global search. By observing the comparison made in table 1, in the case of 1ms of data, method B reduces the FFT complexity for 44.66% in comparing with that of method A. However if the length is 10ms, it only improves the percentage by 5.57%.

C. Half Size Non-Coherent Circular Correlation[3]

This method is also similar with method A, the difference is that in the step 5 of method A, only half of the L(K) and CG(K) is used, thus the IFFT result is 8184 bits. From figure 1, it is easily found that most of the power or information of $l(t)=R_{Fdoppler}(t)\times ca(t)$ is distributed in the first half part (1, 8184). Thus, by using half of the spectrum, only 16.9% is lost.

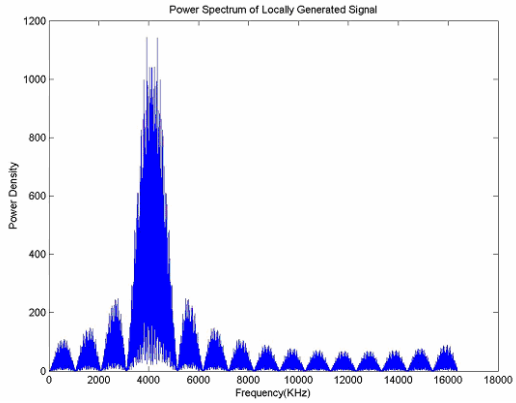

Figure 1. Power Spectrum of $l(t)$

It should be noted that, this method can not be employed in Method B, the reason is shown in the figure 2, wherein without the frequency shift led by the carrier wave, the power spectrum of PRN code alone is distributed equivalent in the first and second half part. Therefore, introducing a Half Size method in B, results in 50% of the power loss.

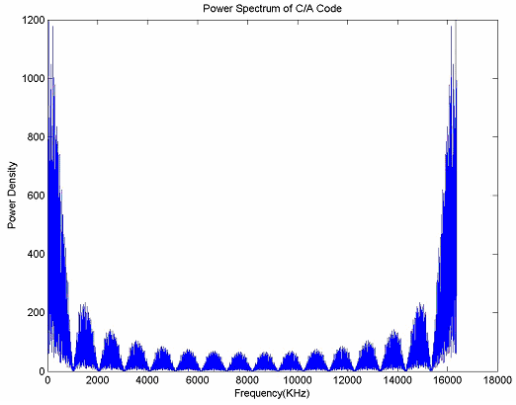

Figure2. Power Spectrum of $ca(t)$

D. Quarter Size Non-Coherent Circular Correlation

This method is the same as method C, with the exception that D only process one quarter of data (from 2047 to 6138 in figure 1) in the step 5, which still contains 69.1% of the total power. The time resolution of this method decreases to 244.38ns.

The reasons why we do not introduce a 1/8 size method (from 3070 to 5115 in figure 1) are that the selecting zone only covers the main lobe and will result in a 44.2% of energy loss, If one considers the Doppler frequency shift, then the loss will be even greater. Besides, a 1/8 size method would deteriorate the time resolution to be 488.8ns or 1/2 chip, which might also make the weak signal acquisition insensitive.

E. Coherent Circular Correlation

Coherent Integration is to coherently acquire successive time slices of data and process them sequentially, not separately. The procedure of a coherent integration method is presented as follows, in the case of n ms of integration:

1. Coherently generate 12*n+1 $R_{Fdoppler}(t)$ for n ms with a dopper frequency range between -6000Hz and 6000Hz at the interval of 1000/n Hz.
2. Multiply n ms $R_{Fdoppler}(t)$ with n ms $g(t)$ to generate n ms signal $l(t)$.
3. Locally generate $ca(t)$ and repeat it for n periods.
4. Perform FFT on $l(t)$ and $ca(t)$ to generate L(K) and CA(K).
5. Take conjugate of CA(K) and get CCA(K)
6. Multiply L(K) and CCA(K) and take IFFT to obtain n*16368 complex outputs. This covers one Doppler frequency component and contains n equivalent correlation peaks, the global peak can be found by just searching the first 16368 bits of the result.

The procedure of method E is similar with that in method B. The benefit of this approach, compared with non-coherent method is that since E is a coherent integration, the frequency resolution of which can be improved to 1/n KHz for n ms of integration, which contributes to a S/N gain of 3dB to 10dB for the integration length from 2ms to 10ms. Therefore it is substantially effective in digging out very weak signals.

The calculation complexity, frequency and time resolution of those five methods are summarized in the table 1.

Table 1. Comparison of five acquisition methods

	FFT Complexity For Global Search (all 32 Satellites, n is the integration time)	Frequency Resolution	Time Resolution
A	(417n+416)*FFT(16368)	1KHz	61.10ns
B	(429n+32)*FFT(16368)	1KHz	61.10ns
C	(416+n)*FFT(16368) 416n*IFFT(8184)	1KHz	122.19ns
D	(416+n)*FFT(16368) 416n*IFFT(4092)	1KHz	244.38ns
E	(396n+65)*FFT(16368n)	(1/n)KHz	61.10ns

Based on the comparison made above, though multiple lengths of integration can increase the acquisition gain, it also contributes to a rise of calculation burden. Method E (Coherent Circular Correlation) holds the best acquisition gain also performs highest in output signal to noise ratio, whereas the processing complexity of which is also the highest. Method C (Half Size Non-Coherent Circular Correlation) and D (Quarter Size Non-Coherent Circular Correlation) reduce the calculation burden in comparing with A (Standard Non-Coherent Circular Correlation), which sacrifices the time resolution to be double and four times coarser than the standard approach. However this coarse time resolution is supposed to be improved by comparing with neighboring bins, or it can be rectified in the further tracking process. In considering the frequency resolution, 1KHz is not enough for a successful tracking. Thus refining the frequency is achieved by applying either amplitude comparison method [3], or coherent FFT method [4].

5. Acquisition Threshold Determination

The acquisition threshold is determined based on accumulative noise probability function that the amplitude of the signal should be above the statistical highest peak output noise [5]. The noise sources in the output signal detector constitute Uncorrelated Autocorrelation Interference (UAI), Cross Correlation Interference (CCI) and background noise. As the background noise is overwhelming in comparing with either UAI or CCI. Thus for the purpose of convenience, only the background noise is taken into consideration when calculating the threshold. This calculation should be sufficient in most of the case.

The output noise in I and Q channel is a complex term and can be denoted as $s_{nI}^2 + js_{nQ}^2$, where s_{nI}^2 and s_{nQ}^2 are the variances and also the average power of Gaussian distributed noises N_I and N_Q, since these two values are almost the same, thus the average noise power in the signal detector can be expressed as $s_{nI}^2 + s_{nQ}^2 = 2s_n^2$. Moreover, the noises N_I and N_Q are normal, and the output noise in the signal detector is expressed as $N_{out} = \sqrt{N_I^2 + N_Q^2}$. Therefore, the distribution of the amplitude of N_{out} is Rayleigh. The probability density function and accumulative probability function of Rayleigh is written as:

$$f(n) = \frac{n}{s_n^2}\exp(-\frac{n^2}{2s_n^2}) \quad (2)$$

$$F(n) = \int_n^\infty f(t)dt = \exp(-\frac{n^2}{2s_n^2}) \quad (3)$$

Take method A as an illustration, for 1ms of data length, the average output noise is obtained from the cross correlation between the collected GPS data and invisible PRN codes, the number of which is 24 totally in the case of data used in this paper. $2s_n^2 = 3.1927\times10^5$ (55.04dB) is measured experimentally by averaging the noise power in the cross correlation noise floor. Figure 3 is an overlay of the measured noise histogram (black zigzag) and directly plotted curve applying equation (2) (green line), the ideal match of which proves the feasibility of this assumption.

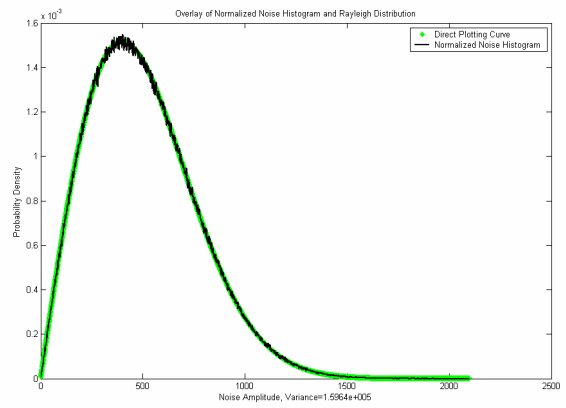

Figure 3. Overlay of normalized noise histogram and Rayleigh probability density function

The peak power of PRN 11 is measured as 2.6470×10^{7} (74.23dB). In order to find the highest statistical noise N_H, a false alarm probability of $\frac{1}{16368\times13\times1000}$ is selected to be the accumulative probability, which means that no more than one false detection is allowed in every 1000 search. Thus, the N_H is calculated from equation (3) as: $F(N_H)=\exp(-\frac{N_H^2}{2s_n^2})=\frac{1}{16368\times13\times1000}$, and the solution is $N_H = 2.4744\times10^{3}$ (67.87dB), which is considered as the threshold value V_T. Thus, the signal of PRN 11 is 6.36 dB above this threshold.

The threshold determined above can be employed in the single search to detect specific satellite or applied in a global search. However if multiple integration is introduced, the threshold varies. In the case of non-coherent integration (A,B,C,D), the increment of the data length, does not actually improve the SNR itself, the gain of which is through smoothing the noise variance, and therefore improving the signal to threshold ratio. Figure 4 depicts the variation of the normalized average noise power (red dot line) and its standard deviation (blue solid line) at different integration times. The decreasing of the standard deviation represents that the maximum noise amplitude is approaching the mean noise.

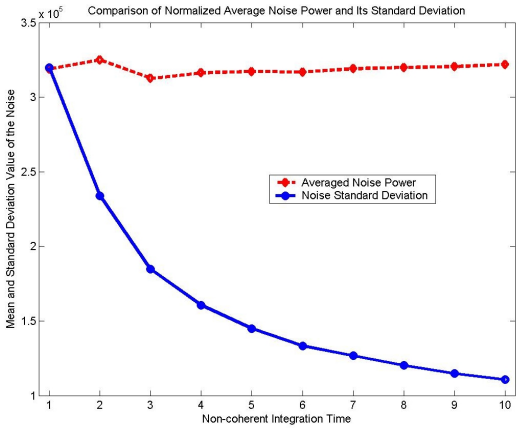

Figure 4. Normalized mean and standard deviation of the output noise

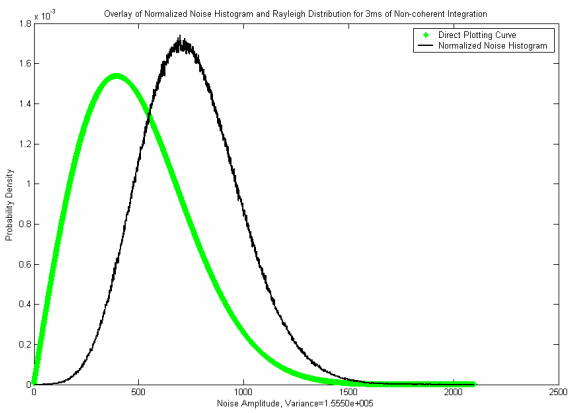

Figure 5. Overlay of noise histogram and Rayleigh probability density function of 3ms of non-coherent integration

Moreover, since the results of processing multiple milliseconds are summed together, the distribution of output noise is no longer in Rayleigh, which is depicted in figure 5. However, one can still consider computing the threshold by using the Rayleigh accumulative probability function, if m ms of integration is used, the peak power of the signal will increase as m times of that of 1ms correlation, but the noise variance used in Rayleigh distribution function only increases as $\sqrt{m}$ times. Thus signal to threshold improves and weak signal will be detected.

Table 2. Threshold Calculation in Method A

	1ms	3ms	5ms	8ms
s_n^2	159640	269330	353730	452770
Max Noise Amplitude	2097.0	2514.5	2904.1	3316.5
Threshold V_T	2474.4	3213.9	3683.2	4167.1

Table 2 presents the threshold calculation results of 1ms, 3ms, 5ms and 8ms of non-coherent integration by using the method A, all of which are 1.44 to 2.13 dB above the measured maximum noise amplitude. This proves the availability and nice performance of this threshold determination method.

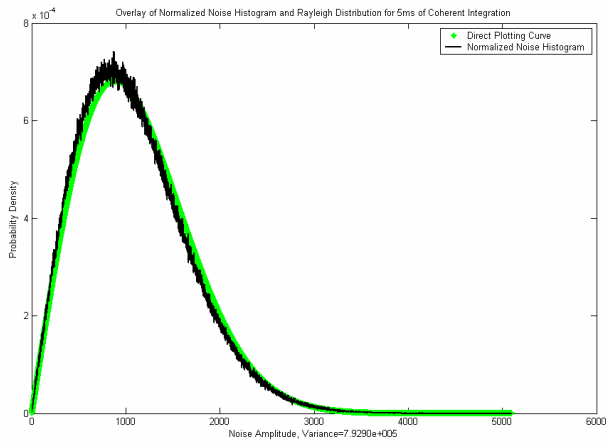

Figure 6. Overlay of noise histogram and Rayleigh probability density function of 5ms of coherent integration

Finally, in the case of coherent integration, figure 6 proves that no matter how many milliseconds are integrated, the output noise is still distributed in Rayleigh, therefore the threshold determination of coherent circular correlation (Method E) is as same as that in 1 ms of method A.

6. Performance Analysis

In the analysis of acquisition performance, method A is taken as the reference, and by integrating 3ms of data, eight satellites are detected as visible, which are PRN 1,3,7,11,19,20,28,31 respectively. In the following tracking process, the fine Doppler frequency and carrier-to-noise ratio (C/No) of each satellite is calculated and listed in the table 3. After evaluation of the C/No, signal in satellite 11 is the strongest and satellite 01 the weakest.

Table 3. Acquisition Result

PRN	Code Phase	Doppler (Hz)	C/No (DB)
01	778	2757.1	38.26
03	13323	-1899.0	39.26
07	3270	3543.4	42.43
11	838	-284.6	47.91
19	6920	-1144.2	41.64
20	13807	3037.0	46.29
28	15500	2839.8	46.21
31	7389	3489.5	42.71

6.1 Speed Comparison

In order to evaluate the processing speed, various integrate times from 1ms to 8ms are applied, for two types of search, global search and single satellite search. All the results are generated in C programming on a Pentium IV 2.80GHz laptop with 768M RAM.

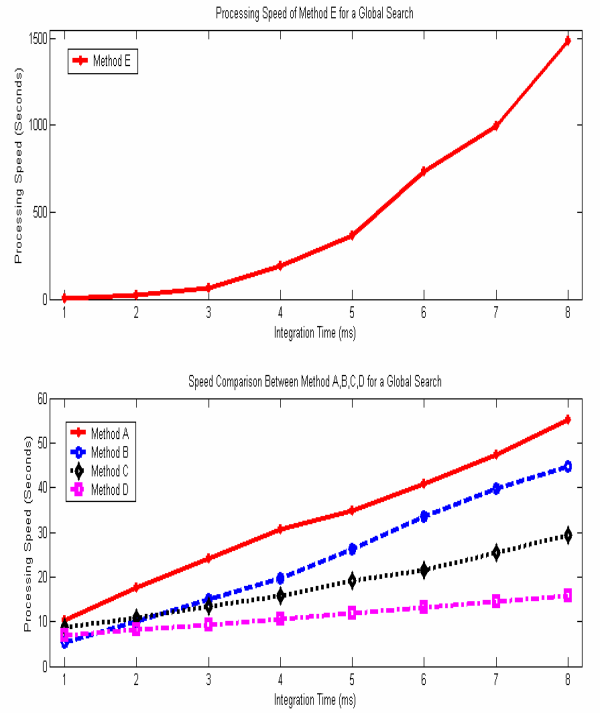

Figure 7. Speed comparison of A, B, C, D and E for a global search

In the case of global search, from the figure 7, it is easily found that the coherent circular correlation (Method E) is much more time consuming than the non-coherent correlation, especially when the integration time is over 3ms. Additionally, the improved non-coherent method (Method B) is superior in processing 1ms data, however as the integration time increases, method D reveals best performance.

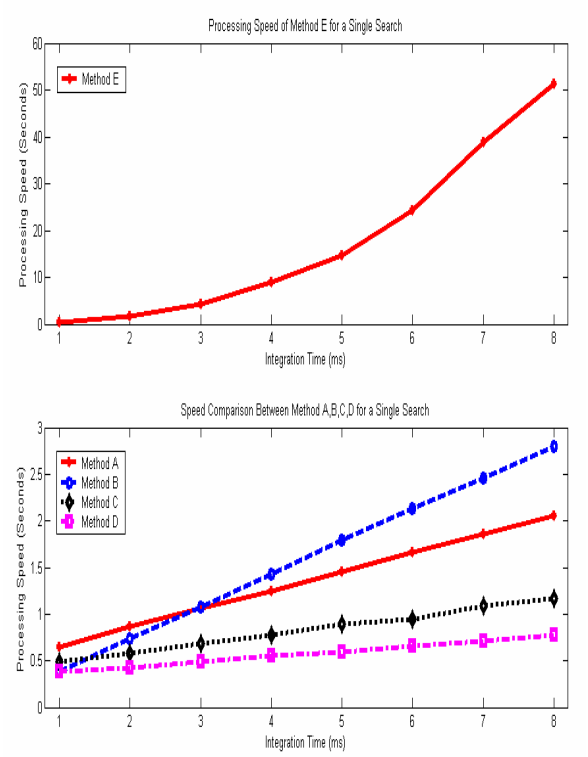

Figure 8. Speed comparison of A, B, C, D and E for a single search

Figure 8 illustrate the case of a single search, in which coherent method is still the most time consuming approach. Comparing the other four non-coherent methods, though method B is still better than A when the time length is less than 3ms, however it is no longer an improved method of A when the integration time surpasses 3ms. Moreover, method D performs as superior as it does in the global search and the increasing slope of which is also small. It should be noted that since the performance of the CPU varies by some factors such as the temperature and sequential working hours, the processing time obtained from the experiment may vary if it is conducted at different times. However, this variation is within a certain range, and will not affect the comparison results presented above.

6.2. Acquisition Gain Comparison

According to the C/No results listed in table 3, signals from satellites 1,31,11 are selected to represent the weak, medium and strong signal, besides, the output signal-to-threshold ratio rather than S/N ratio is applied to evaluate the acquisition gain of various methods. Furthermore, for the purpose of simplicity and without losing generality, integration time of 1ms, 3ms, 5ms and 8ms are chosen to be demonstrated in the following figures:

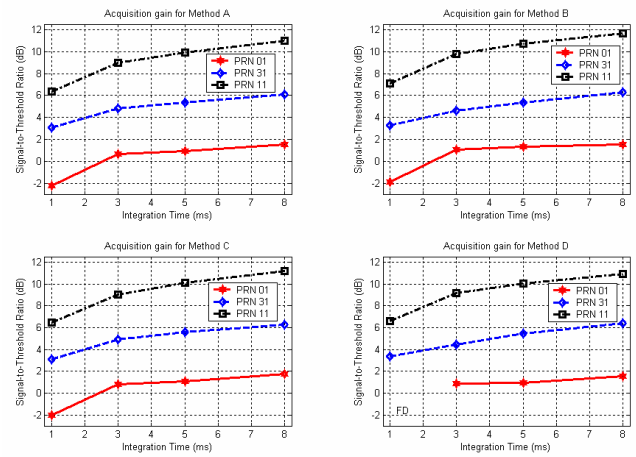

Figure 9. Acquisition Gain for Method A, B, C, D

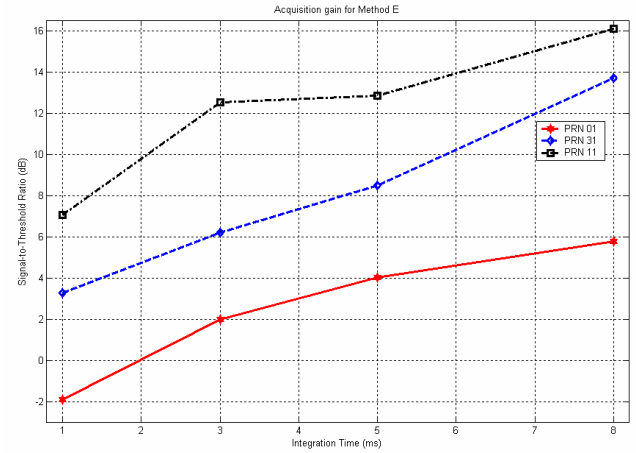

Figure 10. Acquisition Gain for Method E

According to the results depicted in the figures above, when the integration time is only 1ms, the acquisition outputs of PRN 01 are below the predetermined thresholds in all five approaches which indicate that a multiple length of data integration is always required for weak signals. Furthermore, method E, the coherent circular correlation method is overwhelmingly superior in providing the acquisition gain than the rest of the approaches. When processing 1ms of data, method E actually is the same as method B, and by comparing the top right subfigure of figure 9 and figure 10, it is easily found that equal results are obtained from the program. However, as integration times increase, the acquisition gain of E rises dramatically, in the case of 8ms, method E performs a 4.23 dB to 4.41 dB higher signal-to-threshold ratio than that in method B, demonstrating that coherent correlation is much more effective in detecting weak signals.

The acquisition gains in the non-coherent acquisition methods do not reveal a huge gap, except that method B performs slightly better than the other three. Further more, the "FD" mark in the bottom right subfigure of figure 9 means that a false detection or error is found in searching PRN 01, where the peak value found in PRN 01 is not the signal itself but a noise component. The reason is that method D is less sensitive than A in detecting weak signals, since only 69.1% of the total power is applied from the power spectrum in figure 1, resulting in a loss of signal-to-noise ratio. Additionally, the time resolution of method D is four times as coarse as that of method A, which also leads to a insensitive performance of D when processing weak signals. However, if multiple lengths of data are integrated, as demonstrated in figure 9, method D still presents good performance.

7. Conclusion

This paper presents five different acquisition approaches and a practical threshold determination method which is respectively calculated for each approach and independent from hardware configuration. The purpose of this work is to analyze their performance and provide a best scheme for the development of a real-time C/A code Software-based GPS receiver in the University of Tokyo.

By analyzing their acquisition performance, non-coherent method D processes the fastest but is most insensitive in detecting weak signal, coherent method (Method E) is superior for detecting the weak signal, but not applicable in time when the data is too long. Therefore, a balanced application or combination of both coherent and non-coherent approaches is always suggested.

In developing the real time GPS software receiver, several milliseconds of non-coherent acquisition such as B or D is firstly used in the cold start to search globally, and coherent integration can be applied to search the weak signal that is not detected by non-coherent method. Specifically, multiple milliseconds of coherent integration can be significant and effective in the re-acquisition, in which the Doppler frequency is known and the coherent integration at a specified frequency executes quickly.

Acknowledgement

The authors thank Mr. Jens Joergen Nielsen for his arbitrary N FFT C source package [2].

Reference

1. Spilker J. J. and B. Parkingson, Editors, "Global Positioning Systems: Theory and Application", Vol. 1, published by AIAA, 1996, pp.329-407.
2. http://hjem.get2net.dk/jjn/fft.htm
3. James B.Y. Tusi, "Fundamentals of Global Positioning System Receivers, A Software Approach", pp. 133-164.
4. David M Lin and James B.Y. Tsui " A Software Receiver for weak signals", IEEE International Microwave Symposium, May 20-25, 2001
5. David M Lin and James B.Y. Tsui "Acquisition Schemes for Software GPS Receiver", Proceedings of ION GPS 98" September 15-18, 1998, Part 1, pp. 317-326